

**\*\*Volume Title\*\***

*ASP Conference Series, Vol. \*\*Volume Number\*\**

**\*\*Author\*\***

© **\*\*Copyright Year\*\*** *Astronomical Society of the Pacific*

## Narrow Polar Rings versus Wide Polar Ring/Disk Galaxies

E. Iodice

*INAF-Osservatorio Astronomico di Capodimonte, Napoli, Italy*

**Abstract.** In the latest ten years, a big effort has given to study the morphology and kinematics of polar ring galaxies: many steps forward and new discoveries on the structure and formation mechanisms for such systems have been made during this time thanks to high resolution photometric and spectroscopic data. In this paper, I review the latest results obtained for this class of galaxies, from both observational and theoretical studies. I focus on the analysis of the observed properties (e.g., structure, colours, age, metallicity, and kinematics) for narrow and wide polar ring galaxies. In particular, I compare AM 2020-504 and NGC 4650A, which are the two prototypes for narrow and wide polar rings, respectively. I discuss similarities and differences between the two kinds of systems and how they reconcile with the main formation scenarios proposed for this class of galaxies.

### 1. Introduction

Polar ring galaxies (PRGs) are multi-spin systems composed by a central spheroidal component, the host galaxy (HG), and a polar structure which orbits in a nearly perpendicular plane to the equatorial one of the HG. In 1990, Whitmore and collaborators compiled the Catalog of Polar Ring Galaxies, Candidates and Related Objects (PRC), which includes 157 galaxies, where 106 have a well-defined PRG morphology, i.e., the two components (HG and polar structure) are clearly detectable and/or kinematically decoupled. In the rest of the sample, galaxies show a perturbed structure, where the central object has polar or high-inclined feature. Recently, taking advantage of new large data set from surveys, the number of PRG candidates grows up, also at higher redshifts than galaxies in the PRC (Finkelman et al. 2012; Reshetnikov 1997, see also Iodice et al., this volume). In particular, Moiseev et al. (2011) made a new catalogue of PRGs based on the Sloan Digital Sky Survey (SDSS), providing new 275 candidates for polar rings and related objects (see also Smirnova et al., this volume).

For all the included objects in the PRC, the polar structure is identified as a *ring* (Whitmore et al. 1990). Only subsequent studies on the prototype of PRGs, NGC 4650A (Fig. 1), have revealed for the first time that the polar structure in this object has the morphology and kinematics of a *disk*, rather than a ring (see Arnaboldi et al. 1997; Iodice et al. 2002a; Gallagher et al. 2002; Swaters & Rubin 2003). NGC 4650A does not seem the only polar disk galaxy in the universe, but other PRGs show similar characteristics, such as A0136-0801 (PRC A-1) and UGC 9796 (PRC A-6) in PRC and SPRC-27, SPRC-59, and SPRC-69 in the new SDSS-based Polar Ring Catalog (SPRC; Moiseev et al. 2011). Thus, the ‘PRG’ morphological type currently includes both polar rings and polar disks. As I show in this review, they have a different structure (i.e., light

distribution, colors, age, and star motions) and probably a different formation history (but this is still an open issue).

*Why it is interesting to study PRGs?* Given the unique geometry, as suggested by Whitmore et al. (1990), PRGs represent a new way to study galaxy structure and formation. The existence of two orthogonal components of the angular momentum makes the PRGs the ideal laboratory to derive the 3-dimensional shape of the potential (see Combes, this volume). The multi-spin morphology can not be explained by the collapse of a single proto-galactic cloud, but some kind of interaction (galaxy-galaxy or galaxy-environment) need to be invoked in the formation history of these systems. The gravitational interactions are the ‘carrying pillar’ of the cold dark matter (CDM) model for galaxy formation (e.g., Cole et al. 2000), and in this framework, both merger and gas accretion play a major role in building the structure of spheroid and disk (see Conselice, this volume). Thus, PRGs are among the best objects in the universe to study the physics of such processes. In PRGs, as well as for all types of galaxies, the observed morphology, kinematics, structure, and physical properties (i.e., stellar population, gas and dust content, and metallicity) provide the record of the formation mechanism. They result from the relative contribution of each kind of interaction (i.e., merger, accretion, and tidal stripping), from the physical parameters (i.e., mass and gas ratios) and orbital configuration (i.e., trajectory and relative velocity) of the two (or more) interacting systems. All the observed physical quantities listed above need to be reproduced by models of galaxy formation.

In this paper, I review the main observational properties of galaxies with narrow and wide polar rings/disks (Sect. 2), which are the most reliable formation scenarios proposed for PRGs (Sect. 3) and how well they reconcile with the observations (Sect. 4).

## 2. Narrow versus Wide Polar Rings/Disks: Observational Properties

*Morphology and light distribution.* Observations of PRGs show that the morphology of the central HG resembles that of an early-type galaxy (ETG). The polar ring is made up of gas, stars and dust that orbits in a nearly perpendicular plane with respect to central HG. While for most of PRGs the morphology of the HG is always similar to a spheroidal galaxy, the polar structure has different shapes, inclinations and extensions (Whitmore et al. 1990; Moiseev et al. 2011). In *narrow* PRGs the polar ring has a smaller radius with respect to the semi-major axis radius of the HG (see e.g., ESO 415-G26 and AM 2020-504; Iodice et al. 2002b). On the other hand, *wide* polar structures are much more extended than the central component (like A 0136-0801, UGC 7576, and NGC 4650A; Iodice et al. 2002a,b; Cox et al. 2006). In *multiple ring* galaxies several decoupled ring-like structures are observed, and at least one of them is on the polar direction with respect to the central host (e.g., ESO 474-G26; Reshetnikov et al. 2005; Spavone et al. 2012). *Low-inclined rings* are also related objects to the class of PRGs, even if the angle between the HG and ring is less than  $90^\circ$ , reaching also  $45^\circ$  as in NGC 660 (van Driel et al. 1995). Some of the PRG types cited above are shown in Fig. 1. In both narrow and wide PRGs, the surface brightness profiles along the major axis of the HG are well reproduced by a Sérsic law, with an  $n$  exponent that varies in the range  $2 \leq n \leq 4$ . On the contrary, light distribution along the polar structure is quite different in narrow rings with respect to the wide rings/disks: in the first case, the ring appears as a ‘peak’ on the underlying HG surface brightness, while wide po-

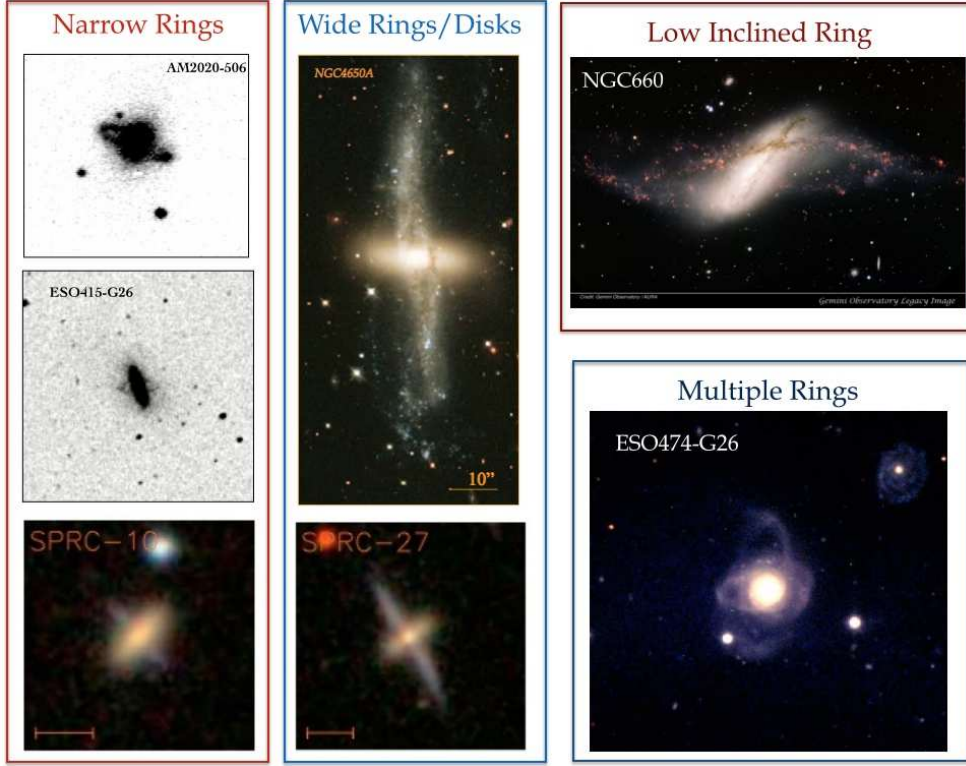


Figure 1. Different morphologies observed for PRGs. Left panels: Narrow PRGs. Central panels: Wide polar rings/disks. Right panels: Low inclined ring (top panel) and multiple rings (bottom panel).

lar rings/disks have an extended exponential-like decreasing profile (Reshetnikov et al. 1994; Iodice et al. 2002a,b,c; Spavone et al. 2012).

*Total luminosity and HI distribution.* Fig. 2 shows the distribution of the total luminosity  $L_B$ , H I mass  $M_{\text{HI}}$  and ratio  $M_{\text{HI}}/L_B$  as function of the relative radial extension of the HG to the polar ring,  $R_{\text{HG}}/R_{\text{PR}}$ , for a sample of PRGs (van Driel et al. 2000, 2002). In this sample, wide PRGs are more numerous than narrow PRGs: this is reasonably due to a selection effect, since wide polar structure in galaxies are easily detectable, and more stable, than the narrow ones. The distribution of all three quantities does not differ between narrow and wide PRGs. For both types of galaxies,  $L_B$  and  $M_{\text{HI}}$  are uniformly distributed and vary in the ranges  $8.8 \times 10^{10} \leq L_B \leq 10.8 \times 10^{10} L_{\odot}$  and  $8 \times 10^{10} \leq M_{\text{HI}} \leq 11 \times 10^{10} M_{\odot}$ . Both narrow and wide PRGs have on average a large amount of H I, that can be 2 or 3 times the total luminosity.

*Stellar kinematics.* As will be discussed in the next two sections, the kinematics of both components (HG and ring/disk) in a PRG is a crucial parameter to discriminate among different formation scenarios for this class of objects, as well as for any morphological type of galaxies. Unfortunately, there are few available spectroscopic data for PRGs that avoid to perform a statistically significant analysis. Anyway, I discuss two different cases: the narrow PRG AM 2020-504 (Fig. 1, left panel) and the wide polar disk galaxy NGC 4650A (Fig. 1, central panel), where the kinematics along the major

Table 1. Colors, ages, and baryonic mass for the narrow PRG AM 2020-504 and wide polar disk galaxy NGC 4650A.

PRG	$B - K$ [mag]	Age [Gyr]	$M_{\text{star+gas}}$ [ $10^9 M_{\odot}$ ]
Host Galaxy			
NGC 4650A	2.86	1 – 3	5
AM 2020-504	3.5	3 – 5	6
Polar Structure			
NGC 4650A	1.6	0.1	12
AM 2020-504	2.7	1	5

axis of the HG and along the polar structure was published. The rotation curve along the ring major axis in AM 2020-504 is consistent with a ring, probably warped towards outer radii (Arnaboldi et al. 1993; Freitas-Lemes et al. 2012). In NGC 4650A, the rotation curve is more similar to that of disks, with a rapid increment in the inner regions followed by a flatter profile at larger radii (Swaters & Rubin 2003). The different kinematics observed for the narrow polar ring and wide polar disk turns to be consistent with the different morphology and light distribution. This is not the case for the central component: even if, in both galaxies, the HG has a spheroidal shape and similar light profile, the observed kinematics is quite different. For both galaxies, along the major axis of the HG rotation velocity increases and reaches  $v \simeq 100 - 130 \text{ km s}^{-1}$  in AM 2020-504, and  $v \simeq 80 - 110 \text{ km s}^{-1}$  in NGC 4650A (Arnaboldi et al. 1993; Iodice et al. 2006). On the other hand, the velocity dispersion profile for AM 2020-504 is very similar to those typically observed in ETGs, peaked in the center ( $\sigma \simeq 260 \text{ km s}^{-1}$ ) and decreasing outwards ( $\sigma \simeq 100 \text{ km s}^{-1}$ , Arnaboldi et al. 1993). For NGC 4650A, the high-resolution Very Large Telescope (VLT) spectroscopy (Iodice et al. 2006) have revealed that the velocity dispersion remains almost constant at  $\sigma \simeq 60 \text{ km s}^{-1}$  out to the last measured data points.

*Colors, ages, and baryonic mass.* Both narrow and wide polar structures are on average bluer and younger than the central HG (Reshetnikov et al. 1994; Iodice et al. 2002a,c), which is free of dust and gas. The large amount of neutral and ionized gas reside in the polar component (e.g., Cox et al. 2006). Colours, ages, and gas content in the HG and polar structure of AM 2020-504 and NGC 4650A are compared in Tab. 1. The  $B - K$  colour, age estimate, and baryonic mass (i.e., mass of stars plus gas) are comparable for the HG in both galaxies. On the other hand, the narrow ring in AM 2020-504 is redder and older than the wide polar disk in NGC 4650A. Furthermore, the baryonic mass in NGC 4650A is 2 times larger than that in AM 2020-504.

*Metallicity in the polar structure.* Recently, the new ongoing field of research on PRGs aims to study the chemical abundances in the polar structure. As I will discuss in the next section, this is another fundamental physical parameter to discriminate among different formation scenarios for this class of objects. The emission lines ([O II],  $H\beta$ , [O III],  $H\alpha$ ) were used to derived oxygen abundance, expressed as  $12 + \log(\text{O}/\text{H})$ , metallicity  $Z$ , and global star formation rate for the polar structure in several PRGs (Eskridge & Pogge 1997; Perez-Montero et al. 2009; Spavone et al.

2010, 2012; Freitas-Lemes et al. 2012; Spavone & Iodice 2013, and Moiseev et al., this volume). In Fig. 3 is shown  $12 + \log(\text{O}/\text{H})$  vs. total  $B$  luminosity estimated for a sample of PRGs, compared with those derived for late-type and disk galaxies. Most of PRGs with narrow and wide polar structures have on average a sub-solar metallicity with  $8.2 \leq 12 + \log(\text{O}/\text{H}) \leq 8.6$  dex, similar to low- $Z$  spirals and high- $Z$  irregular galaxies. There are three PRGs out of this range: two of them have a very low oxygen abundance,  $12 + \log(\text{O}/\text{H}) < 8$  dex, the wide PRG UGC 9796 and the narrow PRG IIZw71 (Spavone et al. 2012; Perez-Montero et al. 2009), and the spindle galaxy NGC 2685 with a metallicity comparable with the typical values for spiral galaxies (Eskridge & Pogge 1997). It seems that there is no significant difference in the metallicity between the narrow polar rings and wide polar rings/disks. Anyway, the sample of PRGs with available measures for oxygen abundances contains too few objects to give a definitive conclusion on this subject, and more data need to be collected.

*Tully-Fisher relation and Faber-Jackson for PRGs.* As I reviewed before, the polar structure in a PRG has very similar properties (e.g., colors, H I content, age, and metallicity) to late-type galaxies, and in the case of the wide polar rings/disks (like NGC 4650A) also the morphology and kinematics. On the other hand, the observed morphology, colors and light distribution of the HG in PRGs are very similar to that of an ETG (elliptical or S0), and, in some cases (like AM 2020-504), also the kinematics.

How PRGs compare with the most important scaling relations for disks and spheroids, i.e., the Tully-Fisher (TF; Tully & Fisher 1977) and Faber-Jackson (FJ; Faber & Jackson 1976) relations? The position of the PRGs with respect to the TF relation for bright disks was investigated by Iodice et al. (2003) and, recently, for a larger sample by Combes et al. (2013). Most PRGs lie on a parallel relation with respect to the TF for spirals, showing larger H I linewidths than expected for the observed total luminosity (Fig. 4, left panel). Numerical simulations suggest that this observational evidence is related to the shape and orientation of the dark halo (DH) in these systems: the larger rotation velocities observed in PRGs can be explained by a flattened DH, aligned with the polar structure (see also Combes, this volume). Furthermore, the new interesting result is that in the  $\log \Delta V - M_B$  plane the narrow and wide PRGs share the same relation, without any segregation effect between the two morphological types.

On the right panel of Fig. 4, PRGs are compared with a sample of ETGs in the plane  $\log \sigma - M_B$ , where  $\sigma$  is the central velocity dispersion of the HG. Differently from what observed for the TF, both narrow and wide PRGs are far from the FJ relation for ETGs, furthermore, it seems that exist a bimodal distribution of PRGs in the plane  $\log(\sigma) - M_B$ , with some HG having higher  $\sigma$  and few others lower  $\sigma$  with respect to spheroids of comparable total luminosity. If this result will be confirmed by using a larger sample of PRGs, it is a relevant observational fact for the formation scenarios.

### 3. Formation Mechanisms for Polar Ring Galaxies

Up to date three main formation scenarios have been proposed for PRGs (see also Combes, this volume). A major dissipative merger, where a PRG results from a ‘polar’ merger of two disk galaxies with unequal mass (Bekki 1998; Bournaud et al. 2005). The tidal accretion of material (gas and/or stars) by outside, where a polar ring/disk may form by 1) the disruption of a dwarf companion galaxy orbiting around an early-type system, or by 2) the tidal accretion of gas stripped from a disk galaxy out-

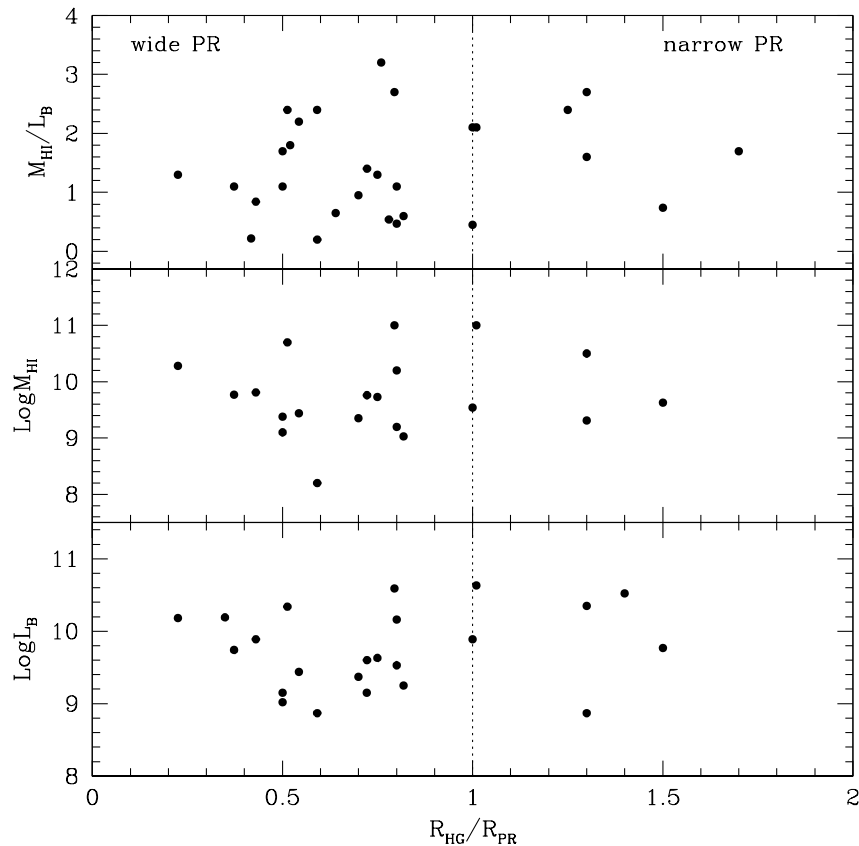


Figure 2. Total luminosity  $L_B$  (bottom panel), H I mass  $M_{\text{HI}}$  (middle panel) and ratio  $M_{\text{HI}}/L_B$  (top panel) as function of the relative radial extension  $R_{\text{HG}}/R_{\text{PR}}$  of HG to polar ring. Data are from van Driel et al. (2000, 2002)

skirts, captured by an ETG on a parabolic encounter (Reshetnikov & Sotnikova 1997; Bournaud & Combes 2003; Hancock et al. 2009). Recently, in the framework of disk formation, the cold accretion of pristine gas along a filament has been proposed as possible formation process for a wide polar disk, like NGC 4650A (Macciò et al. 2006; Brook et al. 2008). Snaith et al. (2012) have revisited the cold accretion scenario, giving more stringent constraints on the structure of the polar disk: this component should have a sub-solar metallicity  $Z = 0.2 Z_{\odot}$ , a flat metallicity gradient, and a younger age ( $< 1$  Gyr) with respect to that of the HG (4–5 Gyr). Furthermore, the DH has its major axis aligned along the polar disk, it is rounder in the inner regions ( $c/a = 0.93$ ) and has an increasing flattening towards larger radii ( $c/a = 0.67$ ).

How one can discriminate among different formation processes? As for any galaxy formation mechanism, the proposed scenarios need to account for the morphology, gas content, star and gas kinematics, and stability. Therefore, the key physical parameters that let to discriminate among the three formation scenarios are 1) the baryonic mass (stars plus gas) ratio between HG and polar structure; 2) the star motions in the HG,

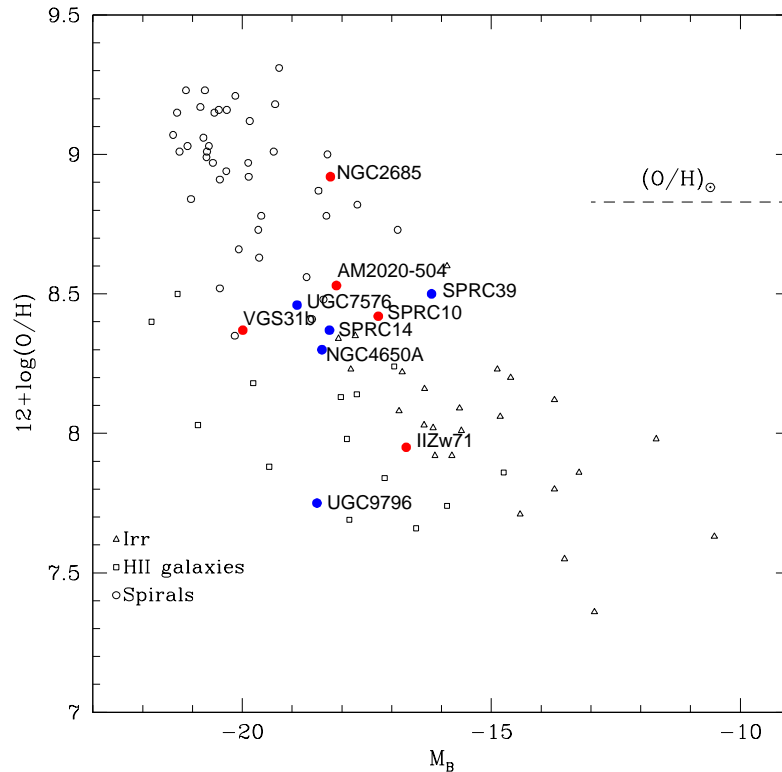


Figure 3. The value of  $12 + \log(\text{O}/\text{H})$  as a function of the total  $B$  luminosity for a sample of PRGs, including the wide polar disk NGC 4650A (Spavone et al. 2010) and the narrow PRG AM 2020-504 (Freitas-Lemes et al. 2012). The red and blue filled points correspond to narrow and wide PRGs, respectively (data are from Perez-Montero et al. 2009; Eskridge & Pogge 1997; Spavone et al. 2010, 2011; Freitas-Lemes et al. 2012; Spavone & Iodice 2013, and Moiseev et al., this volume). The sample of late-type disk galaxies (spiral, H II, and irregular galaxies) are by Kobulnicky & Zaritsky (1999).

i.e., rotation velocity and velocity dispersion; 3) the metallicity and star formation rate in the polar structure.

#### 4. Observations versus Theoretical Predictions

The wide polar disk galaxy NGC 4650A is the best studied PRG, since a large wealth of data are available for this galaxy (see Sect. 2), including H I data (Arnaboldi et al. 1997), near-infrared and optical photometry (Iodice et al. 2002a), and long slit kinematics (Swaters & Rubin 2003; Iodice et al. 2006). Thus, for this object all the key physical parameters were derived and it can be considered the first test case to discriminate among different formation scenarios for PRGs. NGC 4650A has a large baryonic mass in the polar structure, which is equal or even larger than that in the HG (Iodice et al. 2002a, see also Tab. 1). The central spheroid is a rotationally-supported system with

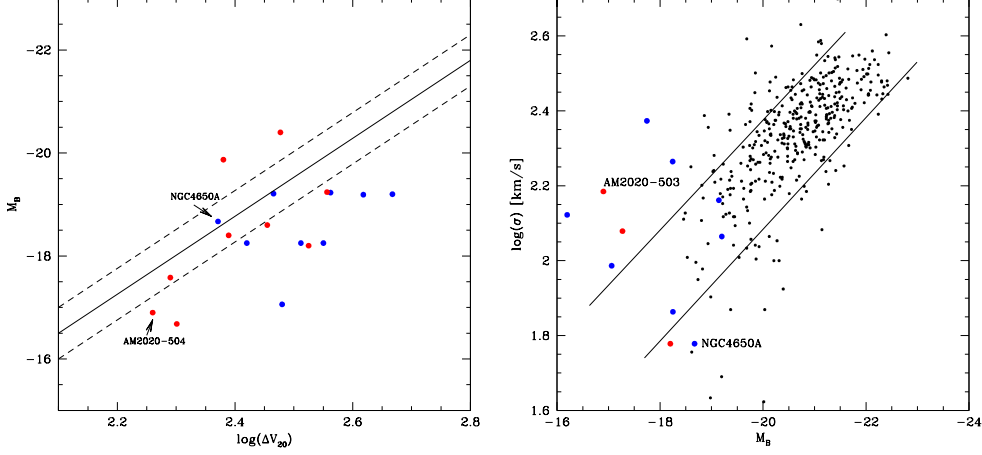


Figure 4. TF and FJ relations for narrow (red circles) and wide (blue circles) PRGs. Left panel: Absolute magnitude in the  $B$  band as a function of the linewidth at 20% of the peak H I-line flux density ( $\Delta V_{20}$ ), for a sample of PRGs (data are from Iodice et al. 2003; Combes et al. 2013), compared with the average TF relation for a sample of spirals from Giovanelli et al. (1997). The solid line is the linear interpolation of the TF relation for spirals and the dashed lines indicate the limit where the 81% disks lie inside. Right panel: Absolute magnitude in the  $B$  band as a function of the central velocity dispersion  $\sigma$  of the HG in a sample of PRGs (data are from Whitmore et al. 1990; Iodice et al. 2006, and Moiseev, priv. comm.). Black points are for the sample of ETGs by Focardi & Malavesi (2012).

the maximum rotation velocity  $v_{\text{rot}} \simeq 80 - 100 \text{ km s}^{-1}$  (Iodice et al. 2006). The polar disk has a sub-solar metallicity  $Z = 0.2 Z_{\odot}$  and there is no metallicity gradient along this component (Spavone et al. 2010, see also Fig. 3). By comparing the above observed quantities with those expected by each formation mechanism, the following conclusions were derived for NGC 4650A: 1) the merging scenario is ruled out because, according to simulations (e.g., Bournaud et al. 2005), it fails to form massive polar disk around an HG with rotation velocities as large as observed along the HG major axis; 2) both the large baryonic mass in the polar structure and its large extension can not be reconciled with a polar disk formed via the gradual disruption of a dwarf satellite galaxy; 3) the tidal accretion could form a such massive and extended polar disk if the donor galaxy has a large amount of gas at large radii (where it is not strongly gravitationally bound) and outside the stellar disk (e.g., Bournaud & Combes 2003); 4) the measured metallicity and its flat gradient, together with the polar disk and HG morphologies, kinematics, gas content, and stellar ages, turn to be consistent with the predictions by Snaith et al. (2012) for a polar disk formed through the accretion of external cold gas from cosmic web filaments (Spavone et al. 2010).

By analyzing the available data for the narrow PRG AM 2020-504 (see Sect. 2), the same analysis done for NGC 4650A can be performed. Observations show that the HG and ring have comparable baryonic mass (Tab. 1); the HG has a high central velocity dispersion along the major axis that decreases outwards, while the rotation velocity increases out to  $\sim 100 - 130 \text{ km s}^{-1}$ ; the ring has similar oxygen abundances to those of low- $Z$  spiral galaxies (Freitas-Lemes et al. 2012, see also Fig. 3). Thus,



taking into account the above observed properties, and the HG morphology, colors, and age which are very similar to those of an ETG, the ring in AM 2020-504 could be reasonably formed through tidal accretion of material from outside by a pre-existing ETG. This process could not modify the global structure of the progenitor accreting galaxy, which remains with a spheroidal morphology and same colors and age. On the contrary, as suggested by the position of AM 2020-504 with respect to the FJ for ETGs (Fig. 4), the kinematics could change: the HG has an higher velocity dispersion of stars with respect to the typical values observed for ETGs of comparable total luminosity. Simulations of galaxy formation show that gravitational interactions and merging affect the observed kinematics of the remnant galaxy (e.g., Bournaud et al. 2005; Naab et al. 2006). This could be also a reasonable explanation for the smaller  $\sigma$  observed in the HG of NGC 4650A in the  $\log \sigma - M_B$  plane (Fig. 4). If the HG was originally a disk (as assumed by the cold accretion scenario proposed by Brook et al. 2008) and thus was characterized by a very low velocity dispersion, the gravitational interaction that let to the formation of the polar disk could have ‘puffed-up’ the disk, which now appears in its final stage as a spheroidal system with a larger  $\sigma$ .

A similar kind of analysis has been performed for other PRGs to test the accretion scenarios versus the merging process (e.g., Reshetnikov et al. 2005; Spavone et al. 2011, 2012; Spavone & Iodice 2013).

## 5. Concluding Remarks

In this paper I reviewed the latest results obtained for PRGs from both observational and theoretical studies. This class of galaxies includes different kind of morphologies, narrow rings, wide polar rings/disks, and related objects (e.g., multiple or low inclined rings). I focused on the analysis of the observed physical properties (e.g., structure, colours, age, metallicity, and kinematics) for narrow and wide PRGs. In particular, I compared AM 2020-504 and NGC 4650A, which are the two prototypes for narrow and wide PRGs, respectively. I discussed similarities and differences between the two kinds of systems and how they reconcile with the main formation scenarios proposed for PRGs. The main results of this analysis are listed below.

- For both narrow and wide PRGs, total luminosity  $L_B$  and H I mass  $M_{\text{HI}}$  are uniformly distributed and vary in the ranges  $8.8 \times 10^{10} \leq L_B \leq 10.8 \times 10^{10} L_\odot$  and  $8 \times 10^{10} \leq M_{\text{HI}} \leq 11 \times 10^{10} M_\odot$ . Both narrow and wide PRGs have, on average, a large amount of H I, that can be 2 or 3 times the total luminosity.
- The HG has similar (spheroidal) morphology, colours, and age in both AM 2020-504 and NGC 4650A, but very different kinematics. In particular, the profile of the stellar velocity dispersion is different. As a consequence, the two galaxies have a different position with respect to the FJ relation for ETGs (see Fig. 4, right panel). This is also observed for other few PRGs which seem to have a bimodal distribution in the  $\log \sigma - M_B$  plane, with some HGs having a larger  $\sigma$  and few others a lower  $\sigma$  with respect to spheroids of comparable total luminosity. This bimodality seems to be independent from the morphological type (narrow or wide PRGs). This result needs to be confirmed with a larger sample of PRGs, since its implications on the formation scenarios for spheroids are quite relevant.

- Contrary to the HGs, the polar structures in narrow and wide PRGs have different morphology, baryonic mass, and kinematics, but, on average, similar oxygen abundance (Fig. 3). NGC 4650A and AM 2020-504 also show different age and colours, being the narrow ring older and redder than the wide polar disk (see Tab. 1). Furthermore, the position of both types of PRGs with respect to the TF relation for spiral galaxies is on average the same, i.e., most PRGs lie on a parallel relation with respect to that for spirals, showing larger H I linewidths than expected for the observed total luminosity (see Fig. 4, left panel).
- The key physical parameters (i.e., baryonic mass, HG kinematics, and metallicity in the polar structure), that let to discriminate among the three formation scenarios suggested for PRGs (see Sect. 3) were derived in several works for some PRGs, including NGC 4650A and AM 2020-504. By comparing them with the predictions from models, one can trace the formation history for each object. In particular, in the case of NGC 4650A the cold accretion of gas along a filament is successfully tested.

All the above results suggest that there is not a unique formation scenario for PRGs, but different mechanisms need to be invoked to explain the whole range of the observed properties for this class of galaxies. As already showed by Bournaud & Combes (2003), the analysis performed in this review confirms that both major merger and tidal accretion scenarios are able to account for the observed morphologies and kinematics of narrow as well as wide polar rings/disks. The simulations of a cold accretion of pristine gas along a filament account for the formation of a polar disk, like NGC 4650A. In the metallicity - luminosity plane (see Fig. 3), there are other PRGs, both narrow and wide polar rings/disks, with similar or even lower oxygen abundance: if the low metallicity is a strong constraint in favour of the cold accretion, may polar rings (not disks!), form through this mechanisms?

**Acknowledgments.** I wish to thank A. Moiseev for providing the unpublished kinematic data for some PRGs of the SPRC catalogue, which turn to be very useful to produce the FJ plot presented in this paper. I would like to warmly thank M. Arnaboldi, D. Bettoni, F. Bournaud, M. Capaccioli, L. Coccato, F. Combes, E. M. Corsini, T. de Zeeuw, K. C. Freeman, J. S. Gallagher, G. Galletta, O. Gerhard, P. Kroupa, A. Moiseev, N. R. Napolitano, R. Saglia, L. S. Sparke, and M. Spavone for the discussions and/or works made together in the last ten years of my career, that gave a huge contribution to my knowledge on the research field presented in this work.

## References

- Arnaboldi, M., Capaccioli, M., Cappellaro, E., Held, E. V. & Sparke, L. S. 1993, *A&A*, 267, 21  
 Arnaboldi, M., Oosterloo, T., Combes, F., Freeman, K. C., & Koribalski, B. 1997, *AJ*, 113, 585  
 Bekki, K. 1998, *ApJ*, 502, L133  
 Bournaud, F., & Combes, F. 2003, *A&A*, 401, 817  
 Bournaud, F., Jog, C. J., & Combes, F. 2005, *A&A*, 437, 69  
 Brook, C. B., Governato, F., Quinn, T., et al. 2008, *ApJ*, 689, 678  
 Cole, S., Lacey, C. G., Baugh, C. M., & Frenk, C. S. 2000, *MNRAS*, 319, 168  
 Combes, F., Moiseev, A., & Reshetnikov, V. 2013, *A&A*, 554, A11  
 Cox, A. L., Sparke, L. S., & van Moorsel, G. 2006, *AJ*, 131, 828  
 Eskridge, P. B., & Pogge, R. W. 1997, *ApJ*, 486, 259  
 Faber, S. M. & Jackson, R. E. 1976, *ApJ*, 204, 668

- Finkelman, I., Funes, J. G., & Brosch, N. 2012, MNRAS, 422, 2386
- Focardi, P., & Malavesi, N. 2012, ApJ, 756, 11
- Freitas-Lemes, P., Rodrigues, I., Faúndez-Abans, M. 2012, MNRAS, 427, 2772
- Gallagher, J. S., Sparke, L. S., Matthews, L. D., et al. 2002, ApJ, 568, 199
- Giovanelli, R., Haynes, M. P., Herter, T., et al. 1997, AJ, 113, 22
- Kobulnicky, H. A., & Zaritsky, D. 1999, ApJ, 511, 118
- Hancock, M., Smith, B. J., Struck, C., Giroux, M. L., & Hurlock, S. 2009, AJ, 137, 4643
- Iodice, E., Arnaboldi, M., Bournaud, F., et al. 2003, ApJ, 585, 730
- Iodice, E., Arnaboldi, M., De Lucia, G., et al. 2002a, AJ, 123, 195
- Iodice, E., Arnaboldi, M., Saglia, R., et al. 2006, ApJ, 643, 200
- Iodice, E., Arnaboldi, M., Sparke, L. S., et al. 2002b, A&A, 391, 103
- 2002c, A&A, 391, 117
- Macciò, A. V., Moore, B., & Stadel, J. 2006, ApJ, 636, L25
- Moiseev, A., Smirnova, K. I., Smirnova, A. A., & Reshetnikov, V. 2011, MNRAS, 418, 244
- Naab, T., Jessit, R., & Burkert, A. 2006, MNRAS, 372, 839
- Perez-Montero, E., Garcia-Benito, R., Diaz, A. I., Perez, E., & Kehrig, C. 2009, A&A, 497, 53
- Reshetnikov, V., 1997, A&A, 321, 749
- Reshetnikov, V. P., Bournaud, F., Combes, F., et al. 2005, A&A, 431, 503
- Reshetnikov, V. P., Hagen-Thorn, V. A., Yakovleva, V. A. 1994, A&A, 290, 693
- Reshetnikov, V. P., & Sotnikova, N. 1997, A&A, 325, 933
- Snaith, O. N., Gibson, B. K., Brook, C. B., et al. 2012, MNRAS, 425, 1967
- Spavone, M., & Iodice, E. 2103, MNRAS, 434, 3310
- Spavone, M., Iodice, E., Arnaboldi, M., Longo, G., Gerhard, O. 2011, A&A, 531, 21
- Spavone, M., Iodice, E., Arnaboldi, M., et al. 2010, ApJ, 714, 1081
- Spavone, M., Iodice, E., Bettoni, D. et al. 2012, MNRAS, 426, 2003
- Swaters, R. A., & Rubin, V. C. 2003, ApJ, 587, L23
- Tully, R. B. & Fisher, J. R. 1977, A&A, 54, 661
- Whitmore B. C., Lucas, R. A., McElroy, D. B., et al. 1990, AJ, 100, 1489
- van Driel, W., Arnaboldi, M., Combes, F. & Sparke, L. S. 2000, A&A, 141, 385
- van Driel, W., Combes, F., Arnaboldi, M., & Sparke, L. 2002, A&A, 386, 140
- van Driel, W., Combes, F., Casoli, F. et al. 1995, AJ, 109, 942